Journal of Alloys and Compounds, 184 (1992) 161–173
JALCOM 178

Crystal and magnetic structure of the permanent magnetic material $Ho_2Fe_{14}C$

Ch. Hellwig and K. Girgis
Institut für Kristallographie und Petrographie, ETHZ, CH-8092 Zürich (Switzerland)

R. Coehoorn and K. H. J. Buschow
Philips Research Laboratories, NL-5600 JA Eindhoven (Netherlands)

P. Fischer
Labor für Neutronenstreuung, ETHZ, CH-5232 Villigen PSI (Switzerland)

J. Schefer
Paul Scherrer Institut, CH-5232 Villigen PSI (Switzerland)

(Received November 17, 1991)

Abstract

Investigations of the compound $Ho_2Fe_{14}C$ by means of X-ray and neutron diffraction as well as by metallographic techniques and differential thermal analysis (DTA) were carried out. $Ho_2Fe_{14}C$ crystallizes in the tetragonal space group $P4_2/mnm$ and is isotypic to $Nd_2Fe_{14}B$. The lattice constants are $a = 8.7537(3)$ Å and $c = 11.8156(6)$ Å at 295 K. The nuclear and magnetic structure of $Ho_2Fe_{14}C$ was investigated by means of neutron diffraction at 673 K (above the Curie temperature T_C), room temperature, 50 K and 10 K. The magnetic moments of the Ho atoms are oriented antiparallel to the magnetic moments of the Fe atoms and lie parallel to the c axis. A predicted spin reorientation at 35 K could neither be proved nor rejected. Measurement of the magnetization curve by means of neutron diffraction yields a T_C of 530 K; DTA measurements yield a T_C of 540 K. The nuclear structure of $Ho_2Fe_{17}C_x$ (Th_2Ni_{17} structure type) has been refined simultaneously since such an impurity phase was present in the sample. The values of the iron moments in $Ho_2Fe_{14}C$ found by means of neutron diffraction were compared with literature data obtained by means of ^{57}Fe Mössbauer spectroscopy and with values derived in the present investigation from augmented spherical wave band structure calculations. There is satisfactory agreement between these sets of data.

1. Introduction

Since the promising group of permanent magnetic materials $R_2Fe_{14}B$ (R = rare earth metal) was discovered in 1984 [1], many investigations of such new ternary compounds have taken place. The magnetic and structural properties of these compounds are reviewed in ref. 2. Another promising group of permanent magnetic materials is that of the isotypic compounds $R_2Fe_{14}C$ [3–7], although their Curie temperatures are slightly lower than those of the corresponding $R_2Fe_{14}B$ systems (*e.g.* 535 K for $Nd_2Fe_{14}C$ [8] compared with 585 K for $Nd_2Fe_{14}B$ [2]). However, the $R_2Fe_{14}C$ compounds

0925-8388/92/$5.00

have the advantage of the presence of a solid state transformation at high temperatures which can be used to obtain high coercivity bulk material without the necessity of employing the powder metallurgical route [2]. The magnetic structures of the compounds $Lu_2Fe_{14}C$ (with only a magnetic iron sublattice) and $Tb_2Fe_{14}C$ (there is also a strong rare earth sublattice present which shows no reorientation tendency) have already been studied [9, 10]. In another recent independent publication [11] the magnetic structures of $R_2Fe_{14}C$ (R≡Lu, Er, Dy) were also determined by neutron diffraction. The aim of the present work is to study the magnetic structure of a compound with a predicted spin reorientation at low temperature (*i.e.* 35 K [12] for $Ho_2Fe_{14}C$) and to understand the magnetic behaviour of the $R_2Fe_{14}C$ group. The Curie temperature T_C is in between that of the $Lu_2Fe_{14}C$ compound and that of the $Tb_2Fe_{14}C$ compound. Bulk magnetization measurements yield a T_C of 516–540 K [7, 13, 14].

2. Experimental details

The $Ho_2Fe_{14}C$ compound was prepared by arc melting from starting materials of at least 99.9% purity. Afterwards the sample was wrapped in tantalum foil and sealed in an evacuated quartz tube. Vacuum annealing was performed subsequently for 6 weeks at 900 °C. The microstructure of the annealed sample was studied by standard metallographic techniques. Microhardness measurements were carried out to prove homogeneity.

X-ray powder photographs were obtained using a Guinier focusing camera (Jagodzinski type) with silicon as internal standard. The intensities were measured by means of an automatic Guinier film scanner.

Neutron diffraction measurements were carried out at a high temperature (673 K) above the Curie point, at room temperature (295 K), at a low temperature (50 K) above the predicted spin reorientation temperature of 35 K and below this temperature at 10 K. The measurements were performed on the multidetector powder diffractometer DMC [15] at the 10 MW reactor Saphir (PSI) with neutrons of wavelength $\lambda = 1.701(2)$ Å. The magnetization curve was measured on the two-axis diffractometer at the reactor Saphir using neutrons of wavelength $\lambda = 2.337(2)$ Å.

3. Results

3.1. Metallographic and X-ray results

Figure 1 shows a micrograph of the $Ho_2Fe_{14}C$ sample. Aggregations of small bright areas are visible in the matrix of the two main phases. These areas are assumed to be free iron while the two main phases are assumed to be $Ho_2Fe_{14}C$ and $Ho_2Fe_{17}C_x$. The dark areas are due to pores and oxides. The microhardness measurements show that this sample is homogeneous. The distribution of the different phases is too fine (see micrograph of Fig.

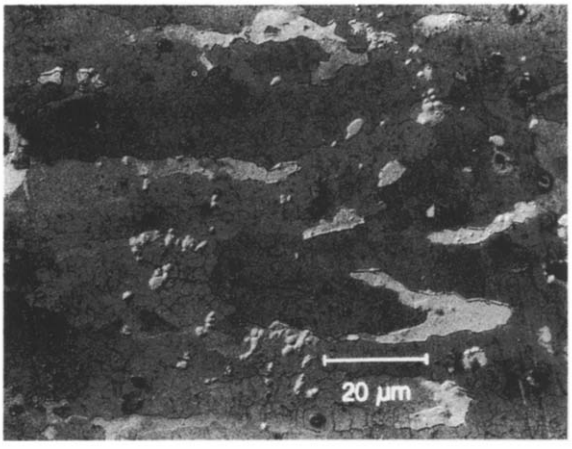

Fig. 1. Micrograph of $Ho_2Fe_{14}C$ sample. The sample was polished with diamond particles (size less than 1 µm) and subsequently electropolished in an ethanol–glycerin–HClO electrolyte. The two main phases are assumed to be $Ho_2Fe_{14}C$ and $Ho_2Fe_{17}C_x$, while the aggregations of small bright areas are assumed to be free iron. The dark areas are due to pores and oxides.

1) to act as inhomogeneities for these measurements. The average value of 10 microhardness measurements amounts to 862(18) HV. The X-ray data show that $Ho_2Fe_{14}C$ crystallizes in the tetragonal space group $P4_2/mnm$ (No. 136) with 68 atoms per unit cell and that the sample also contains a certain amount of $Ho_2Fe_{17}C_x$. The X-ray powder photographs yield lattice constants $a = 8.7537(3)$ Å and $c = 11.8156(6)$ Å at room temperature for $Ho_2Fe_{14}C$.

3.2. Nuclear and magnetic structure

We used as starting parameters those published in ref. 10 for $Tb_2Fe_{14}C$. The rare earth atoms are distributed over two point positions whereas the iron atoms are distributed over six point positions; the carbon atoms occupy one further point position. The second phase, $Ho_2Fe_{17}C_x$, crystallizes in the hexagonal space group $P6_3/mmc$ (No. 194) with $38+2x$ atoms per unit cell. As starting parameters we used those found for the Th_2Ni_{17} type [16]. The rare earth atoms occupy two point positions whereas the Fe atoms are distributed over four point positions; the carbon atoms occupy the point position 6h according to ref. 17. In order to avoid the influence of magnetic intensities on the structure refinement, we studied $Ho_2Fe_{14}C$ at 673 K in the paramagnetic state. The occupation factor of carbon in $Ho_2Fe_{17}C_x$ was refined at this temperature and used for all other temperatures as a fixed value, *i.e.* $Ho_2Fe_{17}C_{0.7}$. The measurements at room temperature and 50 K yield information concerning magnetic saturation. The measurement at 10 K contains information about the behaviour of the magnetic moments below the spin reorientation temperature T_{SR}. The scattering lengths used for holmium, iron and carbon are 0.808×10^{-12}, 0.954×10^{-12} and 0.665×10^{-12} cm respectively [18]. The neutron magnetic form factors were taken from ref. 19 (Ho^{3+}) and ref. 20 (iron). It is worth mentioning that refinements

with the magnetic form factor curve for iron taken from ref. 21 yield higher magnetic moments (ranging from 10% to 35%). The R factors of the fits could be improved by using the magnetic form factor curve in ref. 20.

A three-phase Rietveld refinement [22, 23] was carried out owing to the presence of the $Ho_2Fe_{17}C_x$ phase and traces of free iron. The amount of $Ho_2Fe_{17}C_x$ phase was too small to allow a determination of the magnetic moments of the different point positions; therefore the magnetic moments of the Ho atoms were refined as a single value and the same procedure was adopted for the four iron moments. The orientation of these magnetic moments is perpendicular to the c axis at 10 and 50 K since this delivers significantly better refinements. At 295 K only a slight improvement in the refinement is achieved by the orientation perpendicular to the c axis. The results of the structure refinements are summarized in Tables 1–4 and three patterns are shown in Figs. 2–4.

To obtain the magnetization curve of $Ho_2Fe_{14}C$, the temperature dependence of the integrated neutron intensity of the partial magnetic reflection 110 was measured (Fig. 5). The magnetization M is proportional to $(I_{magn})^{1/2}$ and also to $(1-T/T_C)^{\beta}$:

TABLE 1

Structural parameters of $Ho_2Fe_{14}C$ and $Ho_2Fe_{17}C_x$ at 673 K. The standard deviations of the lattice constants do not include errors from the neutron wavelength, $\Delta\lambda/\lambda$

Atom	Site	Parameter		
		x	y	z
Ho(1)	4f	0.2605(8)	0.2605(8)	0.000
Ho(2)	4g	0.1417(8)	0.8583(5)	0.000
Fe(1)	$16k_1$	0.2256(5)	0.5631(5)	0.1217(3)
Fe(2)	$16k_2$	0.0343(4)	0.3566(5)	0.1757(4)
Fe(3)	$8j_1$	0.0964(5)	0.0964(5)	0.2030(4)
Fe(4)	$8j_2$	0.3160(4)	0.3160(4)	0.2453(5)
Fe(5)	4e	0.000	0.000	0.6080(7)
Fe(6)	4c	0.000	0.500	0.000
C	4g	0.3692(10)	0.6308(10)	0.000
Results of refinement of second phase $Ho_2Fe_{17}C_x$				
Ho(1)	2b	0.000	0.000	0.250
Ho(2)	2d	0.333	0.667	0.750
Fe(1)	4f	0.333	0.667	0.104(1)
Fe(2)	6g	0.500	0.000	0.000
Fe(3)	12j	0.336(1)	0.961(1)	0.250
Fe(4)	12k	0.167(1)	0.334(1)	0.987(1)
C	6h	0.849(5)	0.698(9)	0.250
$B_{Ho}=0.96(8)$ Å^2		$B_{Fe}=0.83(2)$ Å^2		$B_C=1.32(21)$ Å^2
$Ho_2Fe_{14}C$:		$a,b=8.7382(4)$ Å		$c=11.8194(7)$ Å
$Ho_2Fe_{17}C_x$:		$a,b=8.543(1)$ Å		$c=8.3376(7)$ Å
Occupation (C in $Ho_2Fe_{17}C_x$): 23(3)%				Others: 100%
$R_{nuclear}=4.0\%$		$R_{profile}=6.2\%$		$R_{expected}=3.8\%$

TABLE 2

Structural and magnetic parameters of $Ho_2Fe_{14}C$ and $Ho_2Fe_{17}C_x$ at 295 K (magnetic moments of $Ho_2Fe_{14}C$ are fixed parallel to the c axis, magnetic moments of $Ho_2Fe_{17}C_x$ perpendicular to the c axis). The standard deviations of the lattice constants do not include errors from the neutron wavelength, $\Delta\lambda/\lambda$

Atom	Site	Parameter			μ (μ_B)
		x	y	z	
Ho(1)	4f	0.2593(11)	0.2593(11)	0.000	−5.5(1)
Ho(2)	4g	0.1428(10)	0.8572(10)	0.000	−5.1(2)
Fe(1)	$16k_1$	0.2253(7)	0.5627(7)	0.1212(5)	2.3(1)
Fe(2)	$16k_2$	0.0346(6)	0.3583(7)	0.1750(5)	2.3(2)
Fe(3)	$8j_1$	0.0969(6)	0.0969(6)	0.2019(6)	2.2(2)
Fe(4)	$8j_2$	0.3160(6)	0.3160(6)	0.2443(6)	3.1(2)
Fe(5)	4e	0.000	0.000	0.6087(10)	1.7(2)
Fe(6)	4c	0.000	0.500	0.000	2.1(2)
C	4g	0.3706(14)	0.6294(14)	0.000	0.0
Results of refinement of second phase $Ho_2Fe_{17}C_x$					
Ho(1)	2b	0.000	0.000	0.250	−2.3(4)
Ho(2)	2d	0.333	0.667	0.750	−2.3(4)
Fe(1)	4f	0.333	0.667	0.094(2)	3.3(3)
Fe(2)	6g	0.500	0.000	0.000	3.3(3)
Fe(3)	12j	0.337(2)	0.963(1)	0.250	3.3(3)
Fe(4)	12k	0.167(1)	0.333(2)	0.987(1)	3.3(3)
C	6h	0.845(6)	0.691(12)	0.250	0.0
$B_{Ho}=0.58(12)$ Å^2		$B_{Fe}=0.76(2)$ Å^2		$B_C=1.15(29)$ Å^2	
$Ho_2Fe_{14}C$:		$a,b=8.7499(4)$ Å		$c=11.8125(9)$ Å	
$Ho_2Fe_{17}C_x$:		$a,b=8.531(2)$ Å		$c=8.341(1)$ Å	
Occupation (C in $Ho_2Fe_{17}C_x$): 23%				Other: 100%	
$R_{nuclear}=3.9\%$		$R_{magnetic}=5.1\%$		$R_{profile}=6.2\%$	$R_{expected}=4.3\%$

$$M \propto \left[\frac{I_{obs}-I_{nucl}}{I_{nucl}}\right]^{1/2} \propto \left(1-\frac{T}{T_C}\right)^{\beta} \tag{1}$$

The magnetization curve obtained in this way is a superposition of the magnetization curves of the holmium magnetic sublattice and the iron magnetic sublattice. Because of this superposition, it is not possible to determine the critical exponent β for each magnetization curve. The magnetization curve shows a small decrease at 10 K which lies within the standard deviations. In fact the decrease is too small to prove a spin reorientation.

4. Band structure calculations

Band structure calculations were made for the compound $Y_2Fe_{14}C$. This compound does not exist as a stable equilibrium phase but it can be assumed that its 3d electron magnetism is representative for the series of $R_2Fe_{14}C$

TABLE 3

Structural and magnetic parameters of $Ho_2Fe_{14}C$ and $Ho_2Fe_{17}C_x$ at 50 K (magnetic moments of $Ho_2Fe_{14}C$ are fixed parallel to the c axis, magnetic moments of $Ho_2Fe_{17}C_x$ perpendicular to the c axis). The standard deviations of the lattice constants do not include errors from the neutron wavelength, $\Delta\lambda/\lambda$

Atom	Site	Parameter			μ (μ_B)
		x	y	z	
Ho(1)	4f	0.2587(6)	0.2587(6)	0.000	−9.3(1)
Ho(2)	4g	0.1427(6)	0.8573(6)	0.000	−9.3(1)
Fe(1)	$16k_1$	0.2255(6)	0.5628(6)	0.1213(5)	2.3(1)
Fe(2)	$16k_2$	0.0346(5)	0.3583(6)	0.1748(4)	2.6(1)
Fe(3)	$8j_1$	0.0972(6)	0.0972(6)	0.2015(5)	2.4(1)
Fe(4)	$8j_2$	0.3160(5)	0.3160(5)	0.2445(6)	3.1(1)
Fe(5)	4e	0.000	0.000	0.6087(9)	1.9(1)
Fe(6)	4c	0.000	0.500	0.000	2.1(1)
C	4g	0.3709(13)	0.6291(13)	0.000	0.0
Results of refinement of second phase $Ho_2Fe_{17}C_x$					
Ho(1)	2b	0.000	0.000	0.250	−8.8(2)
Ho(2)	2d	0.333	0.667	0.750	−8.8(2)
Fe(1)	4f	0.333	0.667	0.094(2)	2.3(1)
Fe(2)	6g	0.500	0.000	0.000	2.3(1)
Fe(3)	12j	0.337(2)	0.966(1)	0.250	2.3(1)
Fe(4)	12k	0.165(1)	0.331(2)	0.989(1)	2.3(1)
C	6h	0.844(6)	0.689(11)	0.250	0.0
$B_{Ho}=0.53(10)$ Å^2		$B_{Fe}=0.46(2)$ Å^2		$B_C=0.84(26)$ Å^2	
$Ho_2Fe_{14}C$:		$a,b=8.7606(4)$ Å		$c=11.8045(8)$ Å	
$Ho_2Fe_{17}C_x$:		$a,b=8.5262(1)$ Å		$c=8.3533(7)$ Å	
Occupation (C in $Ho_2Fe_{17}C_x$): 23%				Others: 100%	
$R_{nuclear}=3.9\%$		$R_{magnetic}=4.0\%$		$R_{profile}=5.5\%$	$R_{expected}=2.9\%$

compounds. The calculations were performed in the same way as described previously for $Y_2Fe_{14}B$ [24], using the augmented spherical wave (ASW) method and treating exchange and correlation within the local spin density functional approximation. A mesh of 6k points in the irreducible part of the Brillouin zone was used together with lattice dimensions equal to those of $Y_2Fe_{14}B$. Results of the calculations are presented in Table 5, where the local moments of the Fe atoms occupying the six crystallographic sites are defined as the integrated spin densities in the corresponding atomic spheres.

5. Discussion

The compound $Ho_2Fe_{14}C$ crystallizes in the same space group $P4_2/mnm$ as reported previously for $Nd_2Fe_{14}B$ [25]. The lattice constants of $Ho_2Fe_{14}C$ at room temperature determined by X-ray diffraction methods are $a=8.7537(3)$ Å and $c=11.8156(6)$ Å. The lattice constant a decreases with increasing

TABLE 4

Structural and magnetic parameters of $Ho_2Fe_{14}C$ and $Ho_2Fe_{17}C_x$ at 10 K (magnetic moments of $Ho_2Fe_{14}C$ are fixed parallel to the c axis, magnetic moments of $Ho_2Fe_{17}C_x$ perpendicular to the c axis). The standard deviations of the lattice constants do not include errors from the neutron wavelength, $\Delta\lambda/\lambda$

Atom	Site	Parameter			μ (μ_B)
		x	y	z	
Ho(1)	4f	0.2588(7)	0.2588(7)	0.000	−9.0(1)
Ho(2)	4g	0.1431(7)	0.8569(7)	0.000	−9.0(1)
Fe(1)	$16k_1$	0.2257(6)	0.5630(7)	0.1220(5)	2.2(1)
Fe(2)	$16k_2$	0.0340(6)	0.3589(7)	0.1755(5)	2.3(1)
Fe(3)	$8j_1$	0.0972(6)	0.0972(6)	0.2020(6)	2.3(2)
Fe(4)	$8j_2$	0.3152(5)	0.3152(5)	0.2447(6)	3.0(2)
Fe(5)	4e	0.000	0.000	0.6094(10)	1.9(1)
Fe(6)	4c	0.000	0.500	0.000	2.4(1)
C	4g	0.3714(13)	0.6286(13)	0.000	0.0
Results of refinement of second phase $Ho_2Fe_{17}C_x$					
Ho(1)	2b	0.000	0.000	0.250	−7.8(2)
Ho(2)	2d	0.333	0.667	0.750	−7.8(2)
Fe(1)	4f	0.333	0.667	0.095(2)	2.8(1)
Fe(2)	6g	0.500	0.000	0.000	2.8(1)
Fe(3)	12j	0.334(2)	0.965(1)	0.250	2.8(1)
Fe(4)	12k	0.166(1)	0.332(2)	0.989(1)	2.8(1)
C	6h	0.844(6)	0.688(12)	0.250	0.0
$B_{Ho}=0.44(10)$ Å^2		$B_{Fe}=0.55(2)$ Å^2		$B_C=0.79(28)$ Å^2	
$Ho_2Fe_{14}C$:		$a,b=8.7612(4)$ Å		$c=11.8053(8)$ Å	
$Ho_2Fe_{17}C_x$:		$a,b=8.526(2)$ Å		$c=8.353(1)$ Å	
Occupation (C in $Ho_2Fe_{17}C_x$): 23%				Others: 100%	
$R_{nuclear}=4.4\%$		$R_{magnetic}=4.0\%$		$R_{profile}=5.8\%$	$R_{expected}=3.0\%$

temperature from 10 to 295 K by $\Delta a=0.0113(6)$ Å, while c increases by $\Delta c=0.007(1)$ Å, as determined by neutron diffraction measurements under identical experimental conditions. The increase in unit cell volume with decreasing temperature is due to magnetovolume effects, which were discussed in more detail elsewhere [26]. The magnetic moment per formula unit determined by neutron diffraction at 10 K (14.9 μ_B) is found to be higher than the value found by bulk magnetization measurements at 5 K (10.5–10.9 μ_B) [7, 13].

The compound $Ho_2Fe_{17}C_x$ crystallizes in the space group $P6_3/mmc$ (Th_2Ni_{17} structure type [16]). The lattice constants at room temperature determined by neutron diffraction methods (in comparison with the X-ray results for $Ho_2Fe_{14}C$) are $a=8.534(2)$ Å and $c=8.344(1)$ Å. The lattice constant a increases with increasing temperature from 10 to 295 K by $\Delta a=0.004(2)$ Å, while c decreases by $\Delta c=0.012(1)$ Å, as determined by neutron diffraction measurements under identical experimental conditions. The magnetic moments of the Ho atoms in $Ho_2Fe_{17}C_x$ are oriented antiparallel

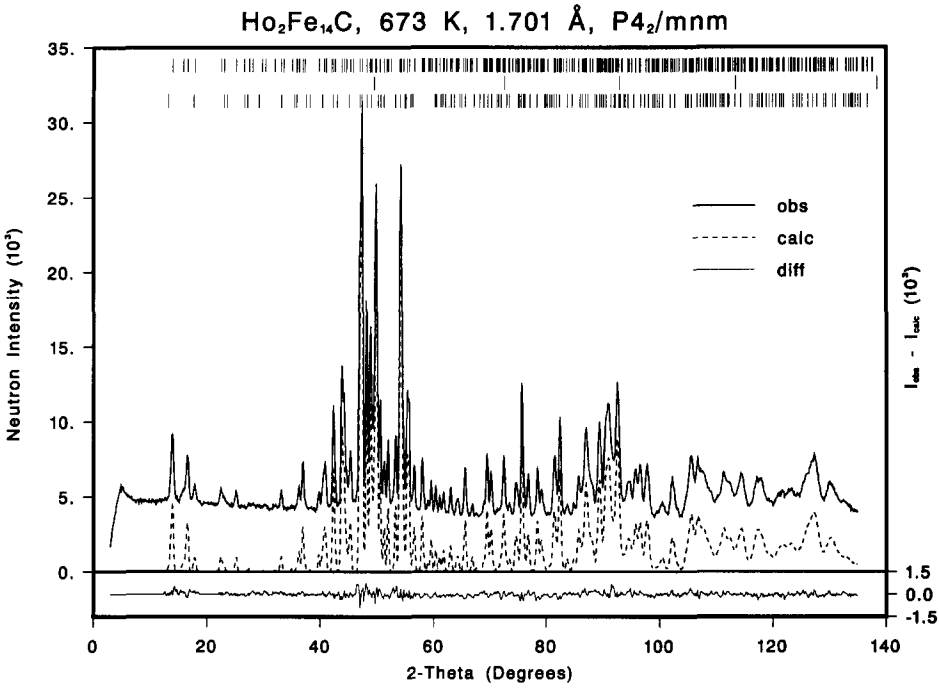

Fig. 2. Observed and calculated neutron diffraction patterns of paramagnetic $Ho_2Fe_{14}C$ at 673 K. The lines at the top indicate the positions of the following reflections: upper row, $Ho_2Fe_{14}C$; middle row, α-Fe; lower row, $Ho_2Fe_{17}C_x$.

to those of the Fe atoms. The easy magnetization direction is always perpendicular to the *c* axis, although the refinement at 295 K is only slightly improved by choosing this magnetization direction.

A spin reorientation of $Ho_2Fe_{14}C$ at 35 K as predicted in ref. 12 could neither be proved nor rejected by the structure refinement or by the measurements of the magnetization curve. The temperature dependence of the latter curve (Fig. 5) shows a small decrease at 10 K which lies within the standard deviations. The structure refinement at 10 K shows a small decrease in the magnetic moments. The *R* factors could not be improved significantly by canting the magnetic moments from the *c* axis by a fixed angle. Furthermore, no "forbidden" reflections were observed, in contrast to the results of investigations made on a single crystal of $Ho_2Fe_{14}B$ [27]. However, the changes in magnetic intensity expected for such processes are very small and may therefore be close to the detectability limit of powder experiments [28].

It is interesting to compare the values found for the various types of iron moments in $Ho_2Fe_{14}C$ with other experimental values and with the results of the band structure calculations described in the previous section.

In Fig. 6(a) we compare the presently determined iron moments with those reported from neutron diffraction studies on $Lu_2Fe_{14}C$ by Yethiraj *et al.* [11]. It is seen that both neutron diffraction studies lead to satisfactory

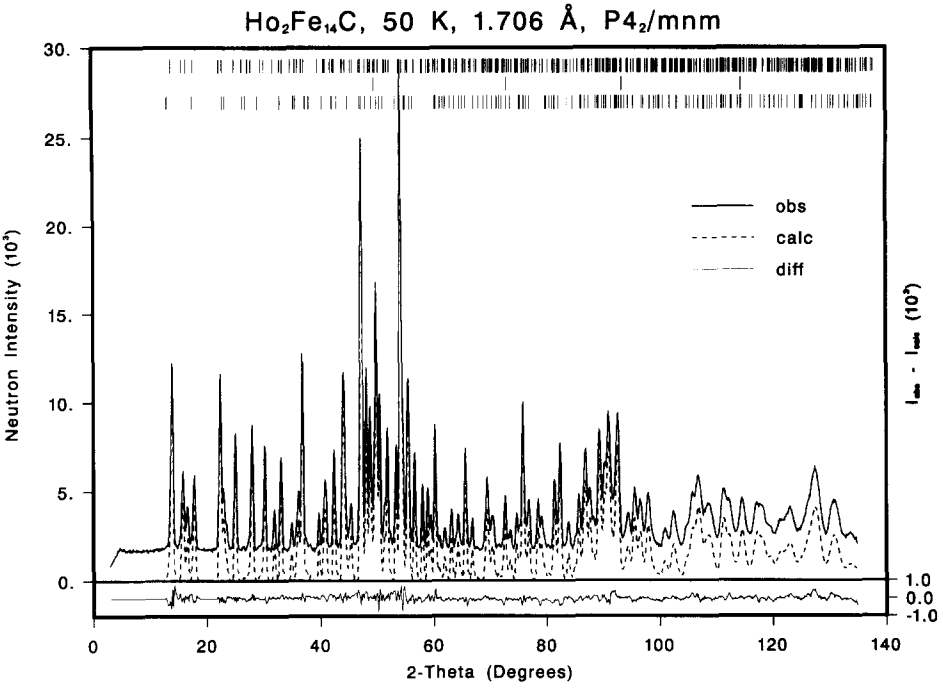

Fig. 3. Observed and calculated neutron diffraction patterns of ferromagnetic $Ho_2Fe_{14}C$ at 50 K. The lines at the top indicate the positions of the following reflections: upper row, $Ho_2Fe_{14}C$; middle row, α-Fe; lower row, $Ho_2Fe_{17}C_x$.

agreement, although the moment values determined for $Lu_2Fe_{14}C$ by Yethiraj *et al.* are slightly higher for several sites than our values.

In Fig. 6(b) we compare our moment values in $Ho_2Fe_{14}C$ with values of the ^{57}Fe hyperfine field reported by Long *et al.* [29] for the same compound. The broken line in the middle part corresponds to the conversion factor 14.5 T μ_B^{-1} commonly employed to transform hyperfine field values into moment values. It is seen that the agreement is also satisfactory. The largest deviation is that of the $8j_2$ site, for which the Mössbauer data suggest a lower moment value than our neutron data. The assignment of the 4e and 4c sites still poses a problem in the interpretation of the ^{57}Fe Mössbauer spectra of $R_2Fe_{14}C$ compounds. The agreement between Mössbauer spectra and neutron data would be improved if the lower hyperfine field were attributed to the 4e site rather than the 4c site in Fig. 6(b). However, making the comparison shown in Fig. 6(b), one should bear in mind that it is still an open question whether it is justified to assume the same proportionality factor between the hyperfine field and moments for all sites [30].

The iron moments derived from the neutron data and those obtained from band structure calculations are compared in Fig. 6(c). There is again good agreement, although the $8j_2$ site was found to have a somewhat higher moment value than predicted from the band structure calculations. A similar situation exists in the corresponding boride compounds [24].

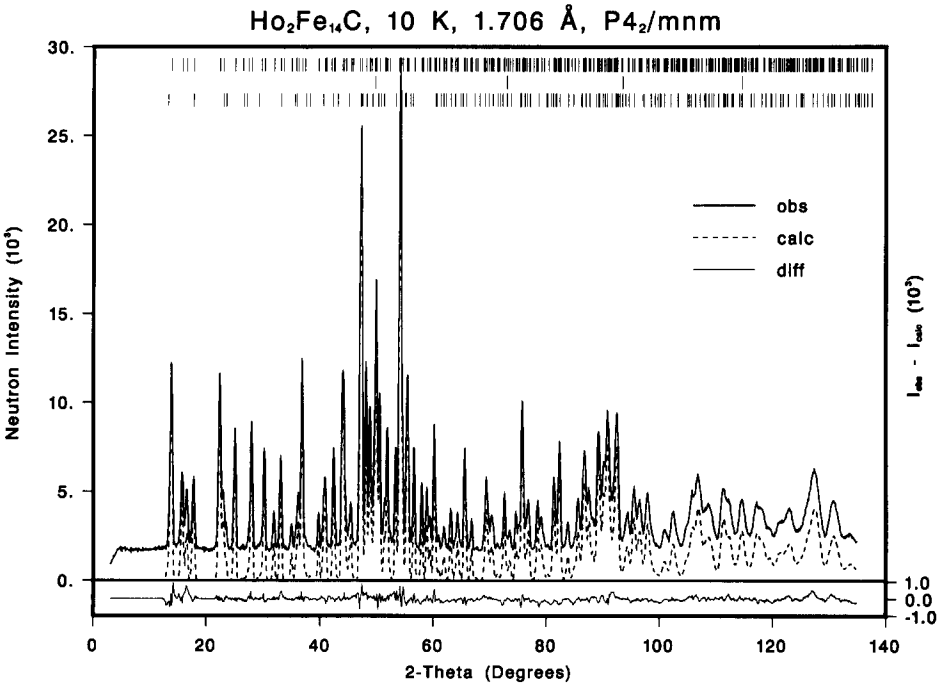

Fig. 4. Observed and calculated neutron diffraction patterns of ferromagnetic $Ho_2Fe_{14}C$ at 10 K. The lines at the top indicate the positions of the following reflections: upper row, $Ho_2Fe_{14}C$; middle row, α-Fe; lower row, $Ho_2Fe_{17}C_x$.

As mentioned above, the magnetic moments of the iron atoms Fe(4) in the $8j_2$ position show a large deviation in comparison with other investigations. Its value determined by the present neutron diffraction study is higher than those determined by Mössbauer spectroscopy for similar compounds ($Ce_2Fe_{14}C$, $Ho_2Fe_{14}C$, $Gd_2Fe_{14}C$ and $Lu_2Fe_{14}C$) [29, 31, 32] but is lower than those for similar compounds determined by neutron diffraction methods ($Nd_2Fe_{14}C$ and $Lu_2Fe_{14}C$) [11, 33].

6. Conclusions

The neutron diffraction data obtained for $Ho_2Fe_{14}C$ in the course of the present investigation confirm that this compound has the tetragonal $Nd_2Fe_{14}B$ structure and orders ferrimagnetically below the Curie temperature with moments oriented along the *c* direction. The magnetic ordering is accompanied by strong magnetovolume effects, the thermal expansion anomalies being mainly restricted to the basal plane. No clear indication of the occurrence of a spin reorientation was obtained.

ASW band structure calculations made in the course of the present investigation show that the values of the magnetic moments of the various types of Fe atoms present in the $Nd_2Fe_{14}B$-type structure are the same in

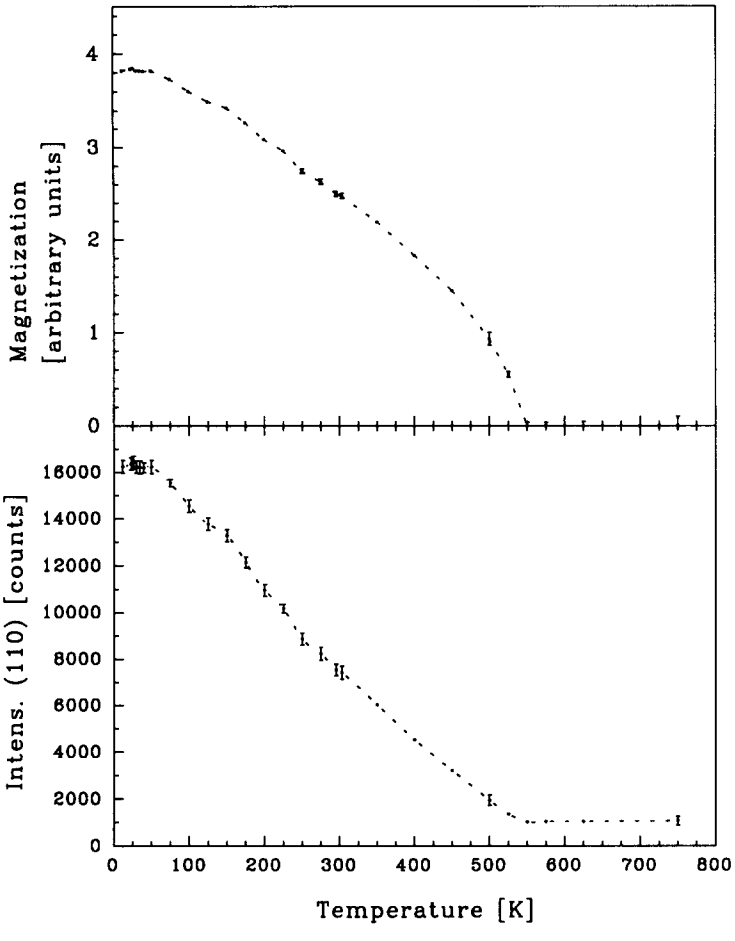

Fig. 5 Magnetization and integrated neutron intensity of the partial magnetic reflection 110 *vs.* temperature; $\lambda = 2.337(2)$ Å.

TABLE 5

Results of ASW calculations for $Y_2Fe_{14}C$ ($\mu_{Fe}(C)$) and $Y_2Fe_{14}B$ ($\mu_{Fe}(B)$). The moment values listed for the boride, which were reported in ref. 24, have been included for comparative purposes

	Fe site					
	$16k_1$	$16k_2$	$8j_1$	$8j_2$	4c	4e
$\mu_{Fe}(C)$ (μ_B)	2.06	2.29	2.21	2.51	2.41	1.94
$\mu_{Fe}(B)$ (μ_B)	2.11	2.31	2.22	2.51	2.40	2.01

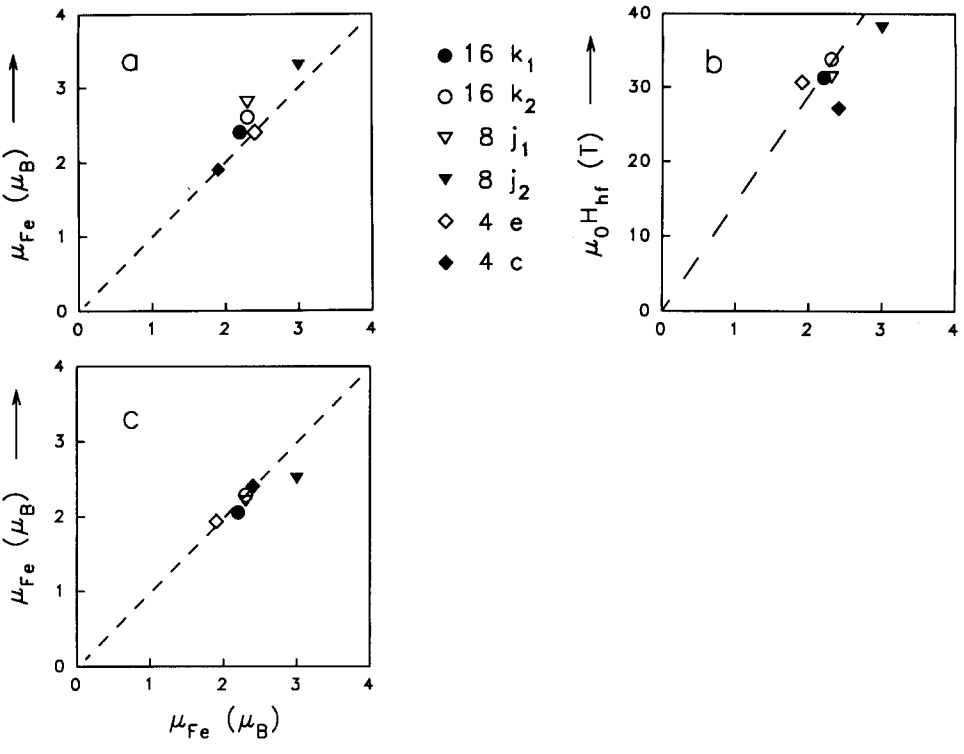

Fig. 6. Comparison of iron moments at 10 K determined in the present work with (a) those reported by Yethiraj *et al.* [11] for $Lu_2Fe_{14}C$, (b) those of the ^{57}Fe hyperfine field for $Ho_2Fe_{14}C$ reported by Long *et al.* [29] and (c) those obtained from band structure calculations.

the borides and carbides to within 3%. We found satisfactory agreement between the moment values determined by neutron diffraction and those derived from the ASW calculations.

Acknowledgments

We wish to thank the workshop group of LNS (especially M. Koch) and the PSI reactor division for support and Professors W. M. Meier and P. Wachter for their interest. This work has been supported by the Swiss National Science Foundation.

References

1 M. Sagawa, S. Fujimura, M. Togawa and Y. Matsuura, *J. Appl. Phys.*, *55* (1984) 2083.
2 K. H. J. Buschow, in E. P. Wohlfarth and K. H. J. Buschow (eds.), *Ferromagnetic Materials*, Vol. 4, North-Holland, Amsterdam, 1988, p. 1.
3 E. P. Marusin, O. I. Bodak, A. O. Tsokol and V. S. Fundamenskii, *Sov. Phys. — Crystallogr.*, *30* (1985) 338.

4 C. Abache and H. Oesterreicher, *J. Appl. Phys.*, *57* (1985) 4112.
5 A. T. Pedziwiatr, W. E. Wallace and E. Burzo, *J. Magn. Magn. Mater.*, *59* (1986) L179.
6 N. C. Liu and H. H. Stadelmaier, *Mater. Lett.*, *4* (1986) 377.
7 M. Gueramian, A. Benzinge, K. Yvon and J. Müller, *Solid State Commun.*, *64* (1987) 639.
8 C. J. M. Denissen, B. D. de Mooij and K. H. J. Buschow, *J. Less-Common Met.*, *142* (1988) 195.
9 Ch. Hellwig, K. Girgis, J. Schefer, K. H. J. Buschow and P. Fischer, *J. Less-Common Met.*, *163* (1990) 361.
10 Ch. Hellwig, K. Girgis, J. Schefer, K. H. J. Buschow and P. Fischer, *J. Less-Common Met.*, *169* (1991) 147.
11 M. Yethiraj, W. B. Yelon and K. H. J. Buschow, *J. Magn. Magn. Mater.*, *97* (1991) 45.
12 F. R. de Boer, R. Verhoef, Z. D. Zhang, B. D. de Mooij and K. H. J. Buschow, *J. Magn. Magn. Mater.*, *73* (1988) 263.
13 F. R. de Boer, Y.-K Huang, Z.-D Zhang, D. B. de Mooij and K. H. J. Buschow, *J. Magn. Magn. Mater.*, *72* (1988) 167.
14 F. Xing and W. W. Ho, *J. Appl. Phys.*, *67* (1990) 4604.
15 J. Schefer, P. Fischer, H. Heer, A. Isacson, M. Koch and R. Thut, *Nucl. Instrum. Methods A*, *288* (1990) 477.
16 W. B. Pearson, *Handbook of Lattice Spacings and Structures of Metals*, Vol. 2, Pergamon, Oxford, 1967, p. 399.
17 P. C. M. Gubbens, A. M. van der Kraan, T. H. Jacobs and K. H. J. Buschow, *J. Magn. Magn. Mater.*, *80* (1989) 265.
18 V. F. Sears, *Methods Exp. Phys. A*, *23* (1986) 521.
19 A. J. Freeman and J. P. Desclaux, *J. Magn. Magn. Mater.*, *12* (1979) 11–21.
20 R. M. Moon, *Int. J. Magn.*, *1* (1971) 219.
21 R. E. Watson and A. J. Freeman, *Acta Crystallogr.*, *14* (1961) 27.
22 H. M. Rietveld, *J. Appl. Crystallogr.*, *2* (1969) 65.
23 A. W. Hewat, *Harwell Rep. AERE-R7350*, 1973.
24 R. Coehoorn, *J. Magn. Magn. Mater.*, *99* (1991) 55.
25 J. F. Herbst and W. B. Yelon, *J. Appl. Phys.*, *60* (1986) 4224.
26 K. H. J. Buschow and R. Grössinger, *J. Less-Common Met.*, *135* (1987) 39.
27 P. Wolfers, S. Miraglia, D. Fruchart, S. Hirosawa, M. Sagawa, J. Batolome and J. Pannetier, *J. Less-Common Met.*, *162* (1990) 237.
28 W. B. Yelon and J. F. Herbst, *J. Appl. Phys.*, *59* (1986) 93.
29 G. J. Long, R. Kulasekere, O. A. Pringle, F. Grandjean and K. H. J. Buschow, *J. Magn. Magn. Mater.*, in press.
30 R. Coehoorn, C. J. M. Denissen and R. Eppenga, *J. Appl. Phys.*, *69* (1991) 6222.
31 T. H. Jacobs, C. J. M. Denissen and K. H. J. Buschow, *J. Less-Common Met.*, *153* (1989) L5.
32 C. J. M. Denissen, D. B. de Mooij and K. H. J. Buschow, *J. Less-Common Met.*, *139* (1988) 291.
33 R. B. Helmholdt and K. H. J. Buschow, *J. Less-Common Met.*, *144* (1988) L33.